

Insight into CO Dissociation in Plasmas from Numerical Solution of a Vibrational Diffusion Equation

Paola Diomede, Mauritius C.M. van de Sanden, and Savino Longo

J. Phys. Chem. C, **Just Accepted Manuscript** • DOI: 10.1021/acs.jpcc.7b04896 • Publication Date (Web): 13 Aug 2017

Downloaded from <http://pubs.acs.org> on August 14, 2017

Just Accepted

“Just Accepted” manuscripts have been peer-reviewed and accepted for publication. They are posted online prior to technical editing, formatting for publication and author proofing. The American Chemical Society provides “Just Accepted” as a free service to the research community to expedite the dissemination of scientific material as soon as possible after acceptance. “Just Accepted” manuscripts appear in full in PDF format accompanied by an HTML abstract. “Just Accepted” manuscripts have been fully peer reviewed, but should not be considered the official version of record. They are accessible to all readers and citable by the Digital Object Identifier (DOI®). “Just Accepted” is an optional service offered to authors. Therefore, the “Just Accepted” Web site may not include all articles that will be published in the journal. After a manuscript is technically edited and formatted, it will be removed from the “Just Accepted” Web site and published as an ASAP article. Note that technical editing may introduce minor changes to the manuscript text and/or graphics which could affect content, and all legal disclaimers and ethical guidelines that apply to the journal pertain. ACS cannot be held responsible for errors or consequences arising from the use of information contained in these “Just Accepted” manuscripts.

Insight into CO₂ Dissociation in Plasmas from Numerical Solution of a Vibrational Diffusion Equation

Paola Diomede^{1,}, Mauritius C. M. van de Sanden¹, Savino Longo²*

¹ *DIFFER – Dutch Institute for Fundamental Energy Research, P.O. Box 6336, 5600 HH Eindhoven, The Netherlands*

² *Dipartimento di Chimica, Universita' degli Studi di Bari, via Orabona 4, 70126 Bari, Italy*

*Corresponding Author

E-mail: p.diomede@diffier.nl

Tel: +31-(0)40-3334-924

Abstract

The dissociation of CO₂ molecules in plasmas is a subject of enormous importance for fundamental studies and in view of the recent interest in carbon capture and carbon-neutral fuels. The vibrational excitation of the CO₂ molecule plays an important role in the process. The complexity of the present state-to-state (STS) models makes it difficult to find out the key parameters. In this paper we propose as an alternative a numerical method based on the diffusion formalism developed in the past for analytical studies. The non-linear Fokker-Planck equation is solved by the time-dependent diffusion Monte Carlo method. Transport quantities are calculated

1
2
3 from STS rate coefficients. The asymmetric stretching mode of CO₂ is used as a test case. We
4
5 show that the method reproduces the STS results or a Treanor distribution depending on the
6
7 choice of the boundary conditions. A positive drift, whose energy onset is determined by the
8
9 vibrational to translational temperature ratio, brings molecules from mid-energy range to
10
11 dissociation. Vibrational-translational energy transfers have negligible effect at the gas
12
13 temperature considered in this study. The possibility of describing the dissociation kinetics as a
14
15 transport process provides insight towards the goal of achieving efficient CO₂ conversion.
16
17
18
19
20
21
22
23

24 Introduction

25
26
27 Plasma-assisted gas conversion techniques are widely considered as efficient building blocks
28
29 in a future energy infrastructure which will be based on renewable but intermittent electricity
30
31 sources. In particular CO₂ dissociation in high-frequency plasmas is of interest in carbon capture
32
33 and utilization process chains for the production of CO₂-neutral fuels¹. In this case, the
34
35 vibrational excitation of the CO₂ molecule plays an important role in the energy efficient non-
36
37 equilibrium dissociation kinetics, however several aspects of the dissociation kinetics in plasmas
38
39 are still unclear.
40
41
42
43

44
45 Dissociation takes place when collisions between molecules and electrons, as well as inter-
46
47 molecular collisions, provide enough energy to lead an already excited molecule into the
48
49 continuum region thereby producing CO and O. The state-to-state (STS) approach^{2,3} allows to
50
51 calculate very accurate reaction rates by considering any vibrational state as an individual
52
53 species. This amounts to solve the so-called Master Equation (ME) for the populations of
54
55 vibrational states^{2,4}: The ME is actually a system of n non-linear ODEs (Ordinary Differential
56
57
58
59
60

1
2
3 Equations) where n is the number of vibrational states considered, with a complex right hand
4
5 side including terms for any possible chemical process, each in the form of a product of the
6
7 values of the vibrational distribution function (VDF) and a temperature dependent rate
8
9 coefficient.
10

11
12
13 The rate coefficients are selected from literature data or, for electron induced processes,
14
15 calculated from the related cross sections and the electron energy distribution function (EEDF).
16
17 The main problem in calculating the VDF for a polyatomic molecule is the large number of
18
19 states leading to a huge number of possible transitions between them. This leads to high
20
21 computational costs and requires large sets of data, most of which not well known.
22
23
24
25

26
27 Specially in the past few years, strong efforts have been devoted to reducing the complexity
28
29 of the kinetics of CO₂ dissociation in plasmas, after many years of inactivity after the works of
30
31 Gordiets and other scientists on lasers kinetics.^{4,5} The current availability of computational
32
33 resources allows the implementation of multi-dimensional fluid models for the description of the
34
35 non-thermal plasmas where CO₂ is activated, but still, the complexity of the plasma/neutral
36
37 chemistry has to be coupled to the flow of the gas/plasma and to the electromagnetic field used
38
39 to generate the plasma. A further complication is given by the presence of multiple time and
40
41 length scales in the kinetics and dynamics of neutral and charged particles.
42
43
44
45

46
47 In the case of CO₂ molecules, three vibrational modes have to be accounted for: symmetric
48
49 stretching, doubly degenerate bending and asymmetric stretching. Usually the formalism
50
51 CO₂(i,j,k) is used where i,j,k are respectively the numbers of quanta in these modes. The
52
53 redistribution of internal energy in CO₂ is the result of a series of elementary processes,
54
55 including VT (vibration to translation) energy exchanges CO₂(i,j,k) + X → CO₂(u,w,v) + X
56
57
58
59
60

1
2
3 where internal energy is partially converted into kinetic energy and VV (vibration to vibration)
4 energy exchanges, $\text{CO}_2(i,j,k) + \text{CO}_2(l,m,n) \rightarrow \text{CO}_2(u,w,v) + \text{CO}_2(a,b,c)$, where most of the
5
6 internal energy is kept as such but redistributed. In this last case energy conservation strongly
7
8
9
10
11 constraints the possible outcomes.

12
13 Armenise *et al.*⁶ considered a complex STS vibrational kinetics for the CO_2 molecule,
14
15 whereby the vibrational modes are not independent, but a reduced model obtained by lowering
16
17 the dissociation energy was used to decrease the number of vibrational states from 9018 to 1224.
18
19 In multi-temperature models (e.g. the one by Kustova *et al.*⁷), each vibrational mode is described
20
21 by a vibrational temperature, but the rapid VV exchange results in the establishment of a
22
23 Boltzmann distribution with a single temperature T_{12} of the combined symmetric and bending
24
25
26
27
28 modes.

29
30
31 In plasma conditions, the detailed discussion in Fridman⁸ (see also Kozák *et al.*³) shows that
32
33 the most important contribution to dissociation is given by vibrational excitation of the
34
35 asymmetric mode. These works focus on the kinetics of this mode. In this light, it is assumed that
36
37 the dominant exchange processes are intra-mode VV where only v changes and corresponding
38
39 VT and eV processes ($e + \text{CO}_2(v) \rightarrow e + \text{CO}_2(v')$) involving the asymmetric stretching mode
40
41 only. To some limited extent the coupling of the asymmetric stretching mode with the other
42
43 modes has been included in Kozák *et al.*³ In this work, although we use a conceptually different
44
45 approach, we are using rate coefficients which are the same as in the aforementioned paper,
46
47 therefore even in these first calculations, our approach inherits the partial coupling with the other
48
49
50
51
52
53
54
55
56
57
58
59
60 modes.

1
2
3 Even with a single mode, the kinetics is still complex and requires high computational cost,
4 especially when used in 2D or 3D models.
5
6

7
8
9 Peerenboom *et al.*⁹ applied a dimension reduction method based on principal component
10 analysis to a STS kinetics model of CO₂ plasmas. Berthelot *et al.*¹⁰ developed a lumped-levels
11 model to avoid solving equations for all individual CO₂ vibrational levels, demonstrating that a
12 3-groups model is able to (more or less) reproduce the asymmetric mode vibrational distribution
13 function of CO₂. Similar procedures were applied in the past to compress the computational
14 requirements of recombining plasma models.¹¹ In the paper by de la Fuente *et al.*¹², a reduction
15 methodology for the STS kinetics was illustrated, whereby the asymmetric stretching vibrational
16 mode levels are lumped within a single group or fictitious species.
17
18
19
20
21
22
23
24
25
26

27
28 A big help in this effort is provided by analytical results obtained in the past describing
29 specific conditions. For example, under the hypothesis that the $i \rightarrow j$ and $j \rightarrow i$ transitions are
30 balanced (i and j are two generic vibrational quantum numbers), and that only intra-mode
31 vibrational exchange processes are important, the Treanor distribution¹³
32
33
34
35
36
37

$$38 \quad P(v) = A \exp\left(-\hbar\omega v / T_v + x_e \hbar\omega v^2 / T_0\right) \quad (1)$$

39
40
41
42 is obtained. In the multi-mode case a more general Treanor-Likal'ter^{14,15} distribution would be
43 appropriate. In Eq. (1), v is the vibrational level quantum number of the asymmetric mode, A is a
44 normalization factor, ω is the vibrational quantum in the energy space, T_v and T_0 are the
45 vibrational and gas temperature, respectively, x_e is the coefficient of anharmonicity. In $P(v)$, T_v
46
47
48
49
50
51
52
53
54
55
56
57
58
59
60 is a parameter related to the internal energy, and describes the population of the first two
vibrational levels.

1
2
3 Since the rate coefficients for VT processes increase dramatically for high vibrational
4 quantum numbers leading to a drop in the high energy region of the VDF, previous studies
5 considered these processes as the main limiting factor to achieve effective molecular
6 dissociation.^{1,2,4} Since, however, dissociation can be represented as boundary conditions of the
7 kinetic problem, it appears natural to elaborate these concepts using a mathematical approach
8 based on partial differential equations. Accordingly, in this paper we reconsider an alternative
9 approach to STS models, presently overlooked being more mathematically demanding with
10 respect to STS models. This is the approach used in analytical theories developed in the
11 70's.^{4,5,8,16-18}

12
13
14
15
16
17
18
19
20
21
22
23
24
25 The approach in question is based on the diffusion approximation^{4,16}, which transforms the
26 ME for the VDF into a Fokker-Planck (FP) equation. Traditionally, in the FP approach as
27 performed by Rusanov *et al.*¹⁶, equations are solved by assuming a condition of null flux, i.e.
28 $J(\varepsilon) = 0$ where J is the total flux of molecules along the energy axis due to VV and VT processes.
29
30
31
32
33
34
35
36
37
38
39
40
41
42
43
44
45
46
47
48
49
50
51
52
53
54
55
56
57
58
59
60
Dissociation, of course, is connected to the boundary condition for $\varepsilon = \varepsilon_{diss}$, where ε_{diss} is the
dissociation limit. Therefore one of the important messages of this paper is the fact that the
condition of null flux, is not consistent with the presence of the dissociation process: CO₂
molecules must experience a net flux from low vibrational levels to the dissociation threshold.
An FP approach opens the possibility to include the non-zero flux boundary condition in a
logical way.

Our approach is to apply to the FP equation numerical solution techniques in order to avoid
the use of approximations which were necessary for the analytical solution; furthermore, we
calculate the transport coefficients which enter into the equation from the best available data³ and
provide continuum interpolations consistent with the diffusion method.

Computational method

The core of the diffusion approach is the replacement of the system of ordinary differential equations describing the kinetics of discrete levels with a single second order partial differential equation, the FP equation. A large literature is found on the derivation of the FP equation.^{4,8,16,19} The use of this equation is justified when transitions between levels close in energy dominate. It implies that molecules are redistributed in energy according to two classes of transport phenomena: 1) the drift, which is deterministic in nature, and moves molecules initially at the same energy at a single new energy after a given time; 2) the diffusion, which is stochastic in nature, and spreads in energy an initial ensemble of particles.

In the diffusion approach, the set of quantum numbers for the vibrational levels is replaced by a continuous energy ε , and two coefficients, a drift coefficient $a(\varepsilon)$ and a diffusion coefficient $b(\varepsilon)$, are introduced instead of the large number of detailed rate coefficients of the STS approach. The drift coefficient measures the speed at which molecules gain (or lose, if negative) energy and therefore is measured in eVs^{-1} ; the diffusion coefficient is one-half of the rate of increase in variance of the energy distribution of an ensemble of test molecules initially at the same energy, therefore it is measured in eV^2s^{-1} . These two coefficients, which are functions of ε , are calculated with standard integral formulas^{8,19} based on kinetic data. This approach, based on two coefficients only, is accurate for chemical processes where the energy exchange is much smaller than the dissociation energy (the “mean free path” must be smaller than the “gradient scale length” in energy space). Accordingly, usually only mono-quantum processes are included into the description. Although few-quantum transitions can be included, multi-quantum jumps are

1
2
3 outside the diffusion approximation. The FP equation is non-linear in the case of CO₂ vibrational
4
5 kinetics due to the nature of the resonant VV process. The problem to be solved has the form:
6
7

$$\frac{\partial}{\partial t} f(\varepsilon, t) = \frac{\partial}{\partial \varepsilon} (-af + (b + cf) \frac{\partial}{\partial \varepsilon} f) + R = -\frac{\partial}{\partial \varepsilon} J + R, \quad (2)$$

8
9
10
11
12
13 where $f(\varepsilon, t)$ is the internal energy distribution of molecules, $a(\varepsilon)$ accounts for the drift due to
14 vibrational excitation by electrons (eV) and VT processes; $b(\varepsilon)$ is the diffusion coefficient due to
15 eV, VT and non-resonant VV processes, $c(\varepsilon)$ is the reduced diffusion coefficient due to resonant
16 VV processes, R is the sub-threshold dissociation term. Molecules always dissociate when $\varepsilon >$
17 ε_{diss} , where ε_{diss} is the dissociation limit, therefore the boundary condition for a solution of Eq.
18 (2) is $f(\varepsilon_{diss}) = 0$.²⁰ Note the difference between assuming a null value of the distribution and a
19 null value of the flux.
20
21
22
23
24
25
26
27
28
29
30
31

32 Both $a(\varepsilon)$, the drift coefficient, and $b(\varepsilon)$, the diffusion coefficient, are calculated from the rate
33 coefficients of different chemical processes using the known formulas from the theory of
34 stochastic processes¹⁹. These rate coefficients are the same used in a STS model (in this work,
35 for example, the ones in the paper by Kozák *et al.*³ were used). According to this theory, the
36 diffusion coefficient is given by $b(\varepsilon) \sim \frac{1}{2} d^2 \nu$ where d is the energy exchanged in a single event
37 and ν is the event frequency per molecule. The drift coefficient $a(\varepsilon)$ is given by $a(\varepsilon) \sim d \nu$. In our
38 case, $d \sim \hbar\omega$, the single process energy exchange calculated by a continuum fit of the energy
39 levels, ν is the chemical reaction rate per molecule given by kn' where k is the rate coefficient
40 and n' is the number density of the reaction partner. Both the $a(\varepsilon)$ and $b(\varepsilon)$ coefficients are the
41 sum of contributions due to corresponding STS processes. For example, the contribution to the
42 drift of mono-quantum VT processes, $\text{CO}_2(v) + \text{M} \rightarrow \text{CO}_2(v-1) + \text{M}$, is given by
43
44
45
46
47
48
49
50
51
52
53
54
55
56
57
58
59
60

$$a_{VT}(\varepsilon) = -(\hbar\omega)k_{VT}(\varepsilon)n_M \quad (3)$$

and the contribution to the diffusion coefficient b due to VV linear processes (VV₁) is given by

$$b_{VV_1}(\varepsilon) = \frac{1}{2}k_{VV_1}(\varepsilon)n_0(\hbar\omega)^2 P_1, \quad (4)$$

where n_0 is the neutral gas density, k_{VV_1} is the rate coefficient for linear VV processes. With respect to the formula (3-127) in Fridman⁸, Eq. (4) has been corrected by a factor P_1 which is the fractional population of the $v = 1$ level in a Treanor distribution

$$P_1 = \frac{P(1)}{P(0)} = \exp\left(-\varepsilon_{01}/T_v + x_e\varepsilon_{01}^2/T_0\hbar\omega\right), \quad (5)$$

where ε_{01} is the energy difference between $v = 0$ and $v = 1$, to account for the fact that the partner of the $X(v) + X(1) \rightarrow X(v+1) + X(0)$ collision is not any molecule, but only the ones in the $v = 1$ state. Only collisions with the $v = 1$ state are included, collisions with higher levels being comparatively less important. The contributions to a and b due to other STS processes are calculated analogously. Since many different values of the rate coefficients may produce nearly the same values of the transport coefficients a and b , in this sense a data reduction is achieved.

The transport coefficients are the sum of the contributions of all chemical processes. A fundamental step is based on the principle that, under the hypothesis of null flux, the Treanor distribution (Eq. (1)) must be recovered. This implies that all the processes contributing to b , also give a contribution to a according to the formula⁸:

$$a(\varepsilon) = -b(\varepsilon) \left(\frac{1}{T_v} - \frac{2x_e \varepsilon}{T_0 \hbar \omega} \right). \quad (6)$$

The first term into the brackets is easily recognized in terms of detailed balance, or fluctuation-dissipation relation¹⁹, while the second one introduces the effect of the anharmonicity parameter x_e and the gas temperature T_0 which may differ from T_v in the non-equilibrium case.

In the continuum formulation it is simple to account for detailed balance. While in the STS approach a list of relations must be satisfied by the VV rate coefficients, in the continuum approach it is sufficient to include an additional term into the expression of the drift coefficient. In this way, following the analytical approach, it can be seen that the Treanor distribution is obtained if the vibrational flux

$$J = af - b \frac{\partial}{\partial \varepsilon} f \quad (7)$$

is set equal to zero (compare with Eq. (1.13) in Rusanov *et al.*¹⁶ and Eq. (13) in Brau¹⁸). The proposed approach in this paper generalizes that based on assuming $J = 0$. In fact, although this approximation has been useful in the past, it is actually not realistic, since molecules eventually dissociate, and dissociation begins an irreversible diffusion from sub-threshold energies to the threshold energy, implying the presence of a nonzero flux in vibrational energy space. In order to avoid this approximation, the FP equation can be solved by a numerical approach for which the assumption of $J = 0$ is not required.

Several numerical methods are applicable to the solution of the FP equation in the context of our approach: in this paper we use a diffusion Monte Carlo method already applied in the past to

1
2
3 similar problems.²¹ This method is based on the short-time propagator of the drift-diffusion
4
5 equation (Eq. (2)) which is given by
6
7

$$8 \quad G(\varepsilon + \xi, h) = \frac{1}{\sqrt{4\pi b h}} e^{-\frac{(\xi - ah)^2}{4bh}}, \quad (8)$$

9
10
11
12
13
14 i.e. the Green function of the Eq. (2) for constant $a(\varepsilon)$ and $b(\varepsilon)$ and neglecting boundary
15 conditions (hence approximated for short time)²², where h is a numerical time step. The choice of
16
17 the time step is based on the requirement that the average energy shift is much less than ε_{diss} , say
18
19 $\varepsilon_{diss}/100$, while a criterion for the convergence of the solution was to check that the steady-state
20
21 for the function f was reached. The solution of Eq. (2) at time $t+h$ is calculated from the solution
22
23 at time t using the following convolution equation²²
24
25
26
27

$$28 \quad f(\varepsilon, t+h) = \int G(\varepsilon + \xi, h) f(\varepsilon + \xi, t) d\xi. \quad (9)$$

29
30
31
32
33
34 Eq. (8) is applied to an ensemble of mathematical dots (walkers) each with a “mathematical
35
36 weight” p_i and a specified energy ε_i which represents the VDF when used to estimate
37
38 macroscopic quantities.
39
40
41

42
43 Basically any walker at any time step performs two moves, the first one deterministic and the
44
45 second one stochastic. The first move takes into account drift described by the a coefficient and
46
47 it is simply an energy shift given by $+a(\varepsilon)h$. The second move produces a random shift
48
49 according to the Gaussian distribution of variance $2b(\varepsilon)h$.
50
51
52

53
54 This method allows a simple treatment of boundary conditions and is free from numerical
55
56 diffusion, which means that a Gaussian solution propagates under a constant $a(\varepsilon)$ and null $b(\varepsilon)$ in
57
58
59
60

1
2
3 the exact way, by shifting its center of mass. Since the solution ranges several orders of
4 magnitudes, a variance reduction, based on the Russian roulette method,²³ is implemented to
5 reduce the computational cost.
6
7
8
9

10
11 Non-linear VV processes (VV_n), e.g. $2X(v) \rightarrow X(v-1) + X(v+1)$ are included in a
12 straightforward way. The reduced diffusion coefficient c in Eq. (2) is given by
13
14 $(1/2)k_{v,v-1}^{v,v+1}(\hbar\omega)^2$. In a time-dependent approach, f is known from previous calculations, and
15 using Eq. (2) c is calculated and summed as a non-linear contribution to the coefficient b in Eq.
16
17
18
19
20
21
22 (7).
23
24

25 Sub-threshold dissociation processes are described by the term R in Eq. (2). This term has the
26 form $R = -k'n'$, where k' is the corresponding rate coefficient, and has dimensions [1/time].
27 Therefore sub-threshold dissociation is included by a removal process of the walker, with
28 probability $p = 1 - \exp(-Rh)$. For both this process and the threshold process, the removed walkers
29 are redistributed randomly in order to keep the normalization constant.
30
31
32
33
34
35
36

37 The function f must be normalized appropriately if STS rate coefficients are used to calculate
38 the non-linear diffusion coefficient c . This is also useful in order to compare the results of the
39 diffusion approach to STS calculations. The STS populations are attributed to levels which are
40 limited in number and the populations of such levels sum to n_0 , the total number density of
41 molecules, while the normalization of f is based on its integral in the $(0, \epsilon_{diss})$ range. An
42 appropriate normalization can be formulated based on the equilibrium case where the population
43 of each STS level is given by the Boltzmann distribution, therefore its value for $v = 0$ is given by
44 n_0/Z , Z being the partition function. The corresponding continuous function has a value of n_0/T_v
45
46
47
48
49
50
51
52
53
54
55
56
57
58
59
60 (the energy is defined in such a way that the energy for the $v = 0$ level is zero): This means that

all energies are scaled down by the zero-point energy of the considered degree of freedom. Therefore, the appropriate normalization is established by setting

$$\int_0^{\varepsilon_{\text{dis}}} f(\varepsilon) d\varepsilon = n_0 \frac{T_v}{Z}. \quad (10)$$

In such a way, the level populations are matched in the equilibrium case. In this equation, Z (expressed in m^{-3}) is actually a cut-off partition function, i.e. the sum of the populations of the very first levels is a Boltzmann distribution at the temperature T_v . The exact number of levels > 2 is immaterial at normal values of T_v , and the difference between this sum and the same calculated using a Treanor distribution is very small. The full function based on the Treanor distribution is not an appropriate choice since the Treanor distribution increases exponentially at high energy.

In order to calculate the a and b coefficients and the c reduced diffusion coefficient due to VV_n processes in the CO_2 molecule case, a continuous polynomial fit of the VV_1 , VV_n and VT rate coefficients at 300 K of the data in Figure 2 in Kozák *et al.*³ as a function of ε (not of the discrete vibrational level index v) is included, as well as a fit of the average energy exchange $\delta\varepsilon(\varepsilon)$ of these processes. For the VV_1 and VV_n processes x_e in eq. (6) was set equal to 5.25×10^{-3} , as in reaction (V8) in Kozák *et al.*³ A functional expression of the rate coefficients $k(\varepsilon)$ as functions of ε is necessary in some expressions for a and b as seen above. To this aim, we have interpolated the corresponding STS rate coefficients after replacing the quantum number v with the corresponding energy as independent variable. The interpolations used in this work are for a fixed T_0 and $\log k$ or k , depending on the case, is fitted as $\sum_{i=0}^4 c_i \varepsilon^i$. To calculate the rate coefficients at different temperatures, the temperature dependencies reported by Kozák *et al.*³ are used. Note that VV'_a and VV'_b processes in Kozák *et al.*³ are here considered as VT processes,

1
2
3 as also recommended in Kozák *et al.*³ Those processes are VV' relaxations between the
4 asymmetric and the first two symmetric mode levels, $\text{CO}_2(\text{v}) + \text{CO}_2 \rightarrow \text{CO}_2(\text{v}-1) + \text{CO}_2(\text{v}_a)$,
5
6 $\text{CO}_2(\text{v}) + \text{CO}_2 \rightarrow \text{CO}_2(\text{v}-1) + \text{CO}_2(\text{v}_b)$.
7
8
9

10
11 As sub-threshold dissociation process we have included reaction (N1) in Kozák *et al.*³, that is
12 $\text{CO}_2(\text{v}) + \text{M} \rightarrow \text{CO} + \text{O} + \text{M}$, where M is any neutral species, assuming for simplicity collisions
13 with CO_2 molecules (in any vibrational state) only. The processes included in the present
14 calculations are summarized in Table 1.
15
16
17
18
19
20
21
22
23
24
25
26
27

28 **Results and Discussion**

29
30
31 In Figure 1, the steady-state solution of Eq. (2) is reported for $n_0 = 2.33 \times 10^{23} \text{ m}^{-3}$, $T_0 = 300 \text{ K}$
32 and three different values of the parameter T_v . The value for the CO_2 number density is based on
33 the results reported on Figure 7 (the 8 ms case) in Kozák *et al.*³ for a power density of 30 W cm^{-3}
34 and a pressure of 2660 Pa which are typical for a CO_2 conversion reactor.^{24,25}
35
36
37
38
39
40

41 As can be seen, the solution for high energies is strongly sensitive to the value of T_v . For
42 comparison, the result of STS calculations by Kozák *et al.*³, based on the same values of the rate
43 coefficients, is reported. The scheme is able to capture the trend of the STS calculations which
44 correspond to a vibrational temperature of 0.19 eV (an estimate based on using the Boltzmann
45 distribution then slightly higher than 0.18 eV here) and therefore is also semi-quantitatively
46 compatible. It is not necessary to match T_v exactly, since this last has a different definition in the
47 discrete and continuum regime. In fact, T_v here is a parameter inside the transport equation,
48
49
50
51
52
53
54
55
56
57
58
59
60

1
2
3 whereas in the STS approach it is deduced *a posteriori* from the $n(v = 1)/n(v = 0)$ population ratio.
4
5 It should be noted that we do not include linear VV collisions with states different than $v = 1$,
6
7 differently from what is done in Kozák *et al.*³ This proves that $v = 1$ is the most important level and
8
9 that with the inclusion of those collisions only, most of the VDF and all the essential features
10
11 obtained with the STS model can be reproduced. Also, we do not include reaction (N2) in Kozák *et*
12
13 *al.*³, that is $\text{CO}_2(v) + \text{O} \rightarrow \text{CO} + \text{O}_2$, since there was no information available on the number
14
15 density of O atoms. This could affect the shape of the VDF in some conditions, as shown in
16
17 Berthelot and Bogaerts.²⁶ However, apparently it is not very important in this case, since we almost
18
19 obtain the same VDF.
20
21
22
23
24

25
26 These calculations allow to perform a first quantitative discussion of the actual transport
27
28 processes of molecules along the vibrational energy scale. In particular, it is possible to
29
30 characterize the drift and diffusion coefficients for different vibrational and gas temperatures and to
31
32 calculate the contribution of the chemical processes to the energy flux J which is connected to
33
34 molecule dissociation.
35
36
37

38
39 Indeed, as shown in Figure 2, our formulation shows the role of the real main factors
40
41 determining the shape of the VDF. Including only VV_1 processes with appropriate boundary
42
43 conditions, the familiar non-equilibrium shape with a long plateau (lower curve) is obtained. Only
44
45 when non physical reflecting boundary conditions (i.e. $J = 0$) at the dissociation threshold are used
46
47 (upper curve) the Treanor distribution appears. This also demonstrates that detailed balance is not a
48
49 sufficient condition to obtain the Treanor distribution, that appears only when the requirement of a
50
51 reflecting boundary condition is selected. With the assumption of reflecting boundary conditions,
52
53 VT processes can play a role and display a qualitatively satisfactory trend (intermediate curve), but
54
55 this trend is still far from the solution of the complete equation, and VT processes play a negligible
56
57
58
59
60

1
2
3 role in the conditions of the present calculations when the appropriate boundary is used. Under the
4 null flux hypothesis, VT processes are found to be essential to retrieve the characteristic shape
5 (including a high slope bulk, a low slope plateau, and high slope tail) of the vibrational
6 distribution.¹⁶ The same concept applies to STS as well, in the sense that a Treanor distribution
7 must result from STS calculations if the dissociation process and VT processes are removed. In
8 Figure 7 in Berthelot and Bogaerts,²⁶ consistently with our general theory, a raise of the VDF is
9 observed removing the dissociation process in STS calculations, although they do not obtain an
10 actual Treanor distribution. These findings are discussed more quantitatively in the next figures.
11
12
13
14
15
16
17
18
19
20
21
22

23 In particular, in Figure 3, the coefficients a and b for the distribution with VV_1 processes only,
24 that reproduces the Treanor distribution in Figure 2, are reported. It can be seen that the b
25 coefficient has a relatively weak dependence on the energy, while the drift coefficient a increases
26 steadily and changes sign at a defined energy depending on the value of the T_v/T_0 parameter. This
27 feature is mostly an effect of the second term inside parentheses of Eq. (6) for a and therefore it is a
28 result of the anharmonicity of the oscillators. This sign change determines most of the shape of the
29 VDF as shown above.
30
31
32
33
34
35
36
37
38
39

40 In Figure 4, the coefficients a and b for the case in Figure 1 that reproduces closely the results in
41 Kozák *et al.*³ ($T_v = 0.18$ eV) are displayed. This figure shows that the diffusion approach produces
42 an effective alternative interpretation of the main phenomena occurring in the vibrational kinetics.
43 The VDF appears as the result of the diffusion in energy space due to VV processes, accelerated in
44 the middle- v region by the drift due to linear VV process. VT processes never play a significant
45 role, their contribution to drift being much lower than VV and VV' processes. It can be seen that
46 the non-linear VV processes are significant only in the low energy region, not an important issue
47 since the low energy part is close to the Treanor distribution.
48
49
50
51
52
53
54
55
56
57
58
59
60

1
2
3 In Figure 5 steady-state results are shown for a higher vibrational temperature of 0.25 eV (n_0
4 and T_0 were not changed with respect to the previous cases). In Figures 6 and 7 the transport
5 coefficients for two of the curves in Figure 5 are shown. In this case, the energy corresponding to
6 the minimum of the Treanor distribution is lower. The plateau of the VDF begins correspondingly
7 at a lower energy. Figure 6, when compared to Figure 3, shows that the main effect of increasing T_v
8 is the shift of the drift coefficient a curve to lower energies while b is not much affected. Again, the
9 second term in Eq. (6) makes the difference.
10
11
12
13
14
15
16
17
18
19

20
21 To better demonstrate this point, Figures 8-9 show the coefficients a and b for different values
22 of the gas and vibrational temperature. These plots show that the “no return” energy level beyond
23 which a molecule most likely dissociates shifts to lower energies when T_0 is reduced. We believe
24 that this is the main reason of the higher energy efficiency found in low T_0 reactors, like the ones
25 exploiting plasma vortexes and expansions¹. In particular, the main parameter appears to be the
26 temperature ratio T_v/T_0 which is related to the energy of the Treanor minimum. Of course, in cases
27 like the ones in Figures 8-9 where the $a(\varepsilon)$ coefficient is always negative, a “no return point” is
28 never reached, but molecules can dissociate anyway due to the random processes of diffusion: the
29 dissociation rate is correspondingly low in such cases.
30
31
32
33
34
35
36
37
38
39
40
41
42

43 As a consequence of the no-return energy concept, VT processes can hardly affect dissociation
44 even under conditions where they could affect the VDF. In fact, high energy molecules are pushed
45 by the drift toward dissociation. VT processes may push molecules backwards, but this will only
46 produce an increase of the VDF to compensate the effect. This situation can change under high
47 temperature conditions where VT processes may become important for vibrational levels below the
48 Treanor minimum.
49
50
51
52
53
54
55
56
57
58
59
60

1
2
3 While these results show the critical role played by the temperature ratio T_v/T_0 as a parameter, it
4 is true that the value of this parameter must be determined (if the case, as a function of time) in a
5 full model. This has been done in recent STS models by including eV processes and their
6 corresponding exothermic, second-kind collisions.^{3,26-28} However, only the very first levels enter
7 the energy balance which determines T_v for a given T_0 , therefore the diffusion model could be
8 integrated in the next future by a very reduced STS energy balance involving only these levels, e.g.
9 three of them. A simple energy balance able to estimate the value of T_v can be established based on
10 the populations of the lowest vibrational levels, even just $v = 0$ and $v = 1$. The balance is based on
11 the eV processes $(v = 0) \rightarrow (v = 1)$ and $(v = 1) \rightarrow (v = 0)$ and the VV_1 process $(v = 1) + (v = 1) \rightarrow$
12 $(v = 2) + (v = 0)$. A simplified steady-state population balance is written in the form:

$$k_{eV01}n_e n(0) = k_{eV10}n_e n(1) + k_{10}^2 n(1)^2 \quad (11)$$

$$n(0) = \frac{n_0}{Z}, \quad n(1) = \frac{n_0}{Z} \exp(-\varepsilon_{01} / T_v + x_e \varepsilon_{01}^2 / T_0 \hbar \omega)$$

27
28
29
30
31
32
33
34 Note that Eq. (11) differs from the usual form of the simplified population balance in using the
35 Treanor instead of the Boltzmann distribution. In view of results of the present study (e.g. Figure
36 1) this is expected to be generally more accurate. Furthermore, in the diffusion approach, T_v is a
37 parameter describing the low energy behaviour of the solution of Eq. (2), therefore, Eq. (1) fixes it
38 unambiguously even for strong non-equilibrium cases. Since, with good approximation, k_{eV01} and
39 k_{eV10} are related by the detailed balance relation (exact in the case of a Maxwellian EEDF), Eq. (11)
40 is readily solved producing T_v as a function of T_e and n_e . In the case of strongly non-equilibrium
41 EEDFs, the usual approach based on the two-term Boltzmann equation^{2,27} can be used to calculate
42 k_{eV01} and k_{eV10} . Eq. (11), therefore, implies that the most important processes controlling the
43 diffusion flux J are the $(v = 0) \rightarrow (v = 1)$ eV transition and the $(v = 1) + (v = 1) \rightarrow (v = 0) + (v = 2)$
44
45
46
47
48
49
50
51
52
53
54
55
56
57
58
59
60

VV process. Furthermore, from the opposite point of view, the diffusion approach could be used to extrapolate, and accelerate considerably, the STS model from the lowest levels upwards. This perspective is very promising for future STS models including detailed coupling to the other two vibrational modes, or even rotational levels.

Conclusions

In this work the diffusion approach was used to study the vibrational kinetics of CO₂ molecules in the context of plasma dissociation. To this aim, the FP equation is solved numerically in order to avoid the use of strong approximations.

Explicit formulas for the transport coefficients a , b and c , this last describing the non-linear effects, are obtained based on the theory of stochastic processes and interpolation of STS rate coefficients. Results are found to be in good agreement with STS calculations in the literature. The results assuming the null flux approximation are reproduced by preventing molecules to dissociate even when reaching ε_{diss} (i. e. a reflecting boundary condition), which, of course, is not physical. Under such conditions, the Treanor distribution is found for a long enough time, a result fully consistent with Treanor's original derivation.¹³ By removing this condition and allowing molecules to dissociate, the plateau in the VDF is obtained even using only linear VV processes. This demonstrates that the essential features of the VDF are mostly a result of the dissociation process which acts like a boundary condition, removing the exceedingly restrictive null flux condition. Our results show that CO₂ molecules reach dissociation threshold under the effect of a positive vibrational drift which onsets at the energy corresponding to the minimum of the Treanor distribution obtained in the null flux case. This conclusion implies that CO₂ molecules are most

1
2
3 likely to dissociate after reaching the no-return energy point which becomes lower when the gas
4 temperature is decreased. This effect, more than the temperature dependence of VT processes, may
5 explain why low gas temperature non-equilibrium plasmas are producing such good results in
6 terms of obtaining high energy efficiency to dissociate molecules. Of course this finding is
7 specific to CO₂, but in perspective our approach can be applied to the dissociation kinetics of other
8 molecules like CH₄ or more complex ones, allowing to determine the role of boundary conditions
9 and the main factors affecting molecular dissociations in such cases.
10
11
12
13
14
15
16
17
18
19

20
21 In this respect, our method requires, in order to calculate appropriate transport coefficients, the
22 determination of very accurate rate coefficients sets specially in terms of consistency of trends
23 (with quantum numbers, with temperature). New rate coefficients sets, furthermore, for the three
24 normal modes, for example involving CO₂(i, j, k) become timely and usable in view of the
25 possibility of a multi-dimensional generalization of the continuum approach.
26
27
28
29
30
31
32
33
34
35

36 **Acknowledgements**

37
38
39 This work is part of the Shell-NWO/FOM initiative ‘Computational sciences for energy
40 research’ of Shell and Chemical Sciences, Earth and Life Sciences, Physical Sciences, FOM and
41 STW, project number 14CSTT02, “Fast and accurate computational approaches to molecular
42 dissociation in non-equilibrium plasmas: the case for CO₂ dissociation”.
43
44
45
46
47
48
49
50
51
52
53
54
55
56
57
58
59
60

References

- (1) Goede, A. and van de Sanden, M. C. M., CO₂-Neutral Fuels, *Europhys. News* **2016**, *47*, 22-26.
- (2) Capitelli, M. (Ed.) *Non-Equilibrium Vibrational Kinetics*, Series: *Topics in Current Physics*; vol. 36, Springer-Verlag: Berlin Heidelberg, 1986.
- (3) Kozák, T.; Bogaerts, A. Splitting of CO₂ by Vibrational Excitation in Non-Equilibrium Plasmas: A Reaction Kinetics Model. *Plasma Sources Sci. Technol.* **2014**, *23*, 045004.
- (4) Gordiets, B. F. *Kinetic Processes in Gases and Molecular Lasers*; Routledge, 1988.
- (5) Gordiets, B. F.; Mamedov, Sh. S. and Shelepin, L. A. Vibrational Kinetics of Anharmonic Oscillators Under Essentially Nonequilibrium Conditions. *Zhurnal Eksperimentalnoi i Teoreticheskoi Fiziki* **1974**, *67*, 1287-1300.
- (6) Armenise, I.; Kustova, E.V. State-to-State Models for CO₂ Molecules: From the Theory to an Application to Hypersonic Boundary Layers. *Chem. Phys.* **2013**, *415*, 269-281.
- (7) Kustova E. V.; Nagnibeda, E. A. Kinetic Model for Multi-Temperature Flows of Reacting Carbon Dioxide Mixture. *Chem. Phys.* **2012**, *398*, 111-117.
- (8) Fridman, A. *Plasma Chemistry*; Cambridge University Press: New York, 2008.
- (9) Peerenboom, K.; Parente, A.; Kozák, T.; Bogaerts, A. and Degrez, G. Dimension Reduction of Non-Equilibrium Plasma Kinetic Models Using Principal Component Analysis. *Plasma Sources Sci. Technol.* **2015**, *24*, 025004.

1
2
3 (10) Berthelot, A.; Bogaerts, A. Modeling of Plasma-Based CO₂ Conversion: Lumping of the
4 Vibrational Levels. *Plasma Sources Sci. Technol.* **2016**, *25*, 045022.
5
6

7
8
9 (11) Benoy, D. A.; van der Mullen, J. A. M.; van de Sanden, M. C. M.; van der Slide, B. and
10 Schram, D. C. Application of a Hybrid Collisional Radiative Model to Recombining Argon
11 Plasmas. *J. Quant. Spectrosc. Radiat. Transfer* **1993**, *49*, 129-139.
12
13

14
15
16 (12) de la Fuente, J. F.; Moreno, S. H.; Stankiewicz A. I. and Stefanidis, G. D. A New
17 Methodology for the Reduction of Vibrational Kinetics in Non-Equilibrium Microwave Plasma:
18 Application to CO₂ Dissociation. *React. Chem. Eng.* **2016**, *1*, 540-554.
19
20
21

22
23
24 (13) Treanor, C. E.; Rich J. W.; Rehm R. G. Vibrational Relaxation of Anharmonic Oscillators
25 with Exchange-Dominated Collisions. *J. Chem. Phys.* **1968**, *48*, 1798-1807.
26
27

28
29
30 (14) Likal'ter, A. A. On the Vibrational Distribution of Polyatomic Molecules. *Prikl. Mekh.*
31 *Tekh. Fiz.* **1976**, *4*, 3 (in Russian).
32
33

34
35
36 (15) Cenian, A. Study of Nonequilibrium Vibrational Relaxation of CO₂, Molecules During
37 Adiabatic Expansion in a Supersonic Nozzle. The Treanor Type Distribution - Existence and
38 Generation. *Chem. Phys.* **1989**, *132*, 41-48.
39
40
41

42
43
44 (16) Rusanov, V. D.; Fridman, A. A.; Sholin, G.V. The Physics of a Chemically Active Plasma
45 with Nonequilibrium Vibrational Excitation of Molecules. *Sov. Phys. Usp.* **1981**, *24*, 447-474.
46
47

48
49
50 (17) Fridman, A.; Kennedy, L. A. *Plasma Physics and Engineering*, 2nd ed.; CRC Press: Boca
51 Raton, FL, 2011.
52

53
54
55 (18) Brau, C. A. Classical Theory of Vibrational Relaxation of Anharmonic Oscillators.
56 *Physica* **1972**, *58*, 533-553.
57
58
59
60

1
2
3 (19) Van Kampen, N. G. *Stochastic Processes in Physics and Chemistry*; Vol. 1, Elsevier:
4
5
6 Amsterdam, The Netherlands, 1992.

7
8
9 (20) Webster, A. G. *Partial Differential Equations of Mathematical Physics*, James Plimpton,
10
11 S. (Ed.), Dover publications: New York, 1955.

12
13
14 (21) D'Ariano, G. M.; Macchiavello, C.; Moroni, S. On the Monte Carlo Simulation Approach
15
16 to Fokker-Planck Equations in Quantum Optics. *Modern Phys. Lett.* **1994**, *8*, 239-246.

17
18
19
20 (22) Pang, T. *An Introduction to Computational Physics*; Cambridge University Press:
21
22 Cambridge, U.K., 1997.

23
24
25 (23) Dupree, S. A. and Fraley, S. K. *A Monte Carlo Primer*, Springer Science + Business
26
27 Media: New York, 2002.

28
29
30
31 (24) den Harder, N.; van den Bekerom, D. C. M.; Al, R. S.; Graswinckel, M. F.; Palomares, J.
32
33 M.; Peeters, F. J. J.; Ponduri, S.; Minea, T.; Bongers, W. A.; van de Sanden, M. C. M.; van Rooij
34
35 G. J. Homogeneous CO₂ Conversion by Microwave Plasma: Wave Propagation and Diagnostics.
36
37 *Plasma Process. Polym.* **2017**, *14*, e1600120.

38
39
40
41 (25) Bongers, W.; Bouwmeester, H.; Wolf, B.; Peeters, F.; Welzel, S.; van den Bekerom, D.;
42
43 den Harder, N.; Goede, A.; Graswinckel, M.; Groen, P. W.; Kopecki, J.; Leins, M.; van Rooij,
44
45 G.; Schulz, A.; Walker, M.; van de Sanden, R. Plasma-Driven Dissociation of CO₂ for Fuel
46
47 Synthesis. *Plasma Process. Polym.* **2017**, *14*, e1600126.

48
49
50
51 (26) Berthelot, A. and Bogaerts, A. Modeling of CO₂ Splitting in a Microwave Plasma: How to
52
53 Improve the Conversion and Energy Efficiency. *J. Phys. Chem. C* **2017**, *121*, 8236-8251.

1
2
3 (27) Capitelli, M.; Colonna, G.; D'Ammando, G. and Pietanza, L. D. Self-Consistent Time
4
5 Dependent Vibrational and Free Electron Kinetics for CO₂ Dissociation and Ionization in Cold
6
7 Plasmas. *Plasma Sources Sci. Technol.* **2017**, *26*, 055009.
8
9

10
11 (28) Aerts, R.; Martens, T.; Bogaerts, A. Influence of Vibrational States on CO₂ Splitting by
12
13 Dielectric Barrier Discharges. *J. Phys. Chem. C* **2012**, *116*, 23257–23273.
14
15
16
17
18
19
20
21
22
23
24
25
26
27
28
29
30
31
32
33
34
35
36
37
38
39
40
41
42
43
44
45
46
47
48
49
50
51
52
53
54
55
56
57
58
59
60

Table 1. Elementary reactions used in the calculations. All rate coefficients are calculated using data in Kozák *et al.*³

Name	Reaction	Note
VV ₁	$\text{CO}_2(1) + \text{CO}_2(v) \rightarrow \text{CO}_2(0) + \text{CO}_2(v+1)$	
VV _n	$\text{CO}_2(v) + \text{CO}_2(v) \rightarrow \text{CO}_2(v-1) + \text{CO}_2(v+1)$	
VT	$\text{CO}_2(v) + \text{CO}_2 \rightarrow \text{CO}_2(v-1) + \text{CO}_2$	^a
Dissociation	$\text{CO}_2(v) + \text{CO}_2 \rightarrow \text{CO} + \text{O} + \text{CO}_2$	^b

^a Sum VT_a + VT_b + VT_c + VV'_a + VV'_b in Kozák *et al.*³

^b Sub-threshold contribution

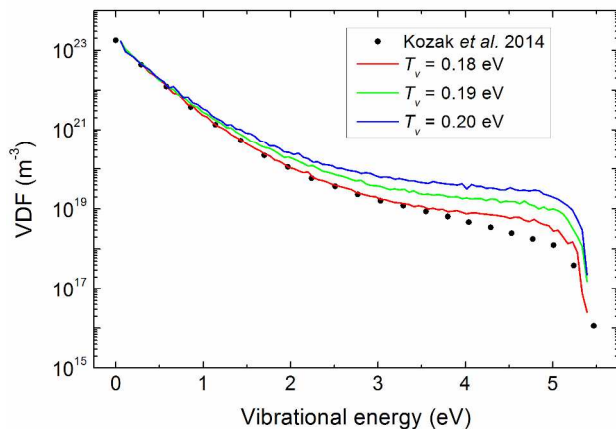


Figure 1. Demonstration that the improved FP approach catches the essential features of the Master Equation. Here the vibrational distribution function of the asymmetric mode levels of the CO_2 molecule is calculated for different values of the vibrational temperature. Results based on expressions of a , b , c and R obtained from rate coefficients in Kozák *et al.*³ Dots represent STS calculations results in Figure 7 (8 ms) in Kozák *et al.*³ for a power density of 30 W cm^{-3} and a T_0 of 300 K, giving a T_v of 0.19 eV, determined from the ratio of the populations in the $v = 0$ and $v = 1$ levels.

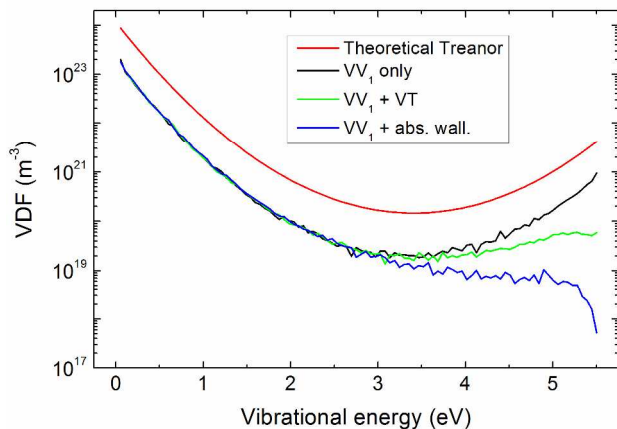


Figure 2. Vibrational distribution functions for $n_0 = 2.33 \times 10^{23} \text{ m}^{-3}$, $T_0 = 300 \text{ K}$ and $T_v = 0.19 \text{ eV}$, obtained for different choices of the boundary condition and processes: VV_1 processes only (black line), VV_1 and VT processes (green line) and absorbing wall boundary condition (blue line). The theoretical Treanor distribution function (red line, shifted upwards for better representation purposes) is also shown.

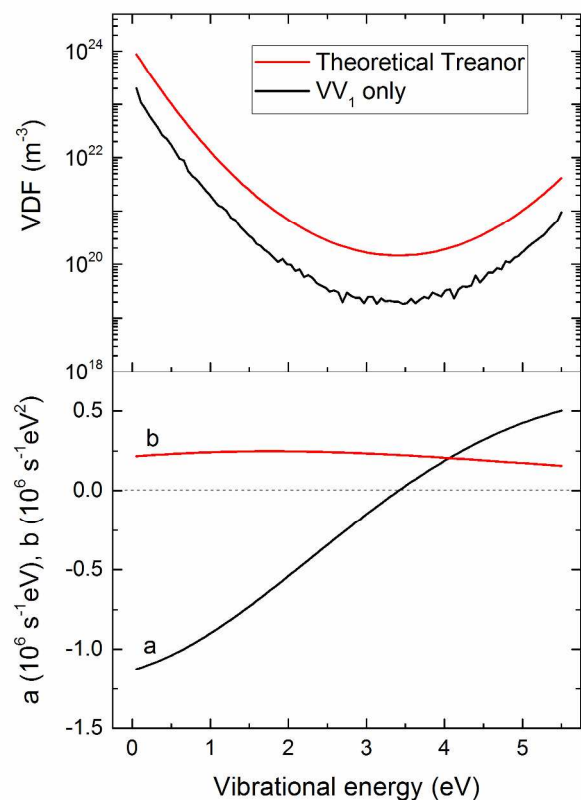


Figure 3. Vibrational distribution function with VV_1 processes only, that reproduces the Treanor distribution for $T_v = 0.19$ eV and $T_0 = 300$ K (see Figure 2) (top) and corresponding coefficients a and b (bottom). In the top panel, the theoretical Treanor distribution function (shifted upwards for better representation purposes) is also shown.

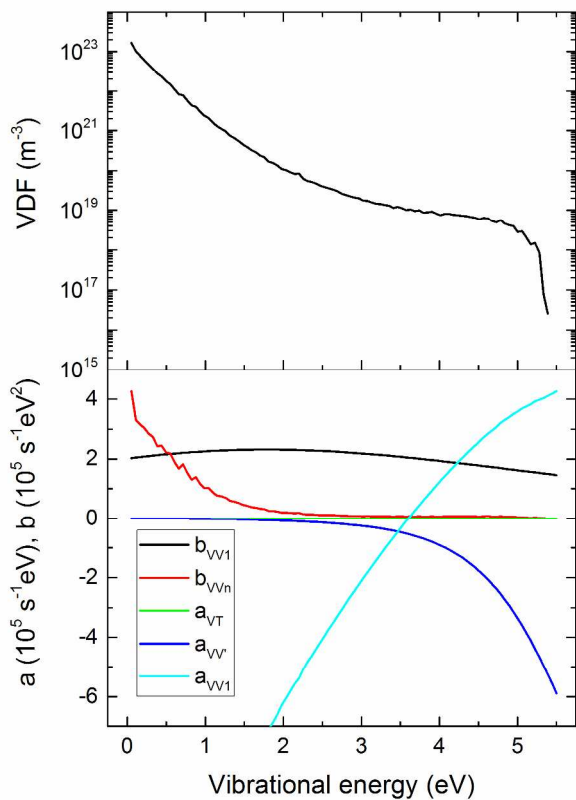


Figure 4. Vibrational distribution function for the case closer to the results in Kozák *et al.*³ ($T_v = 0.18$ eV and $T_0 = 300$ K, see Figure 1) (top) and corresponding coefficients a and b (bottom).

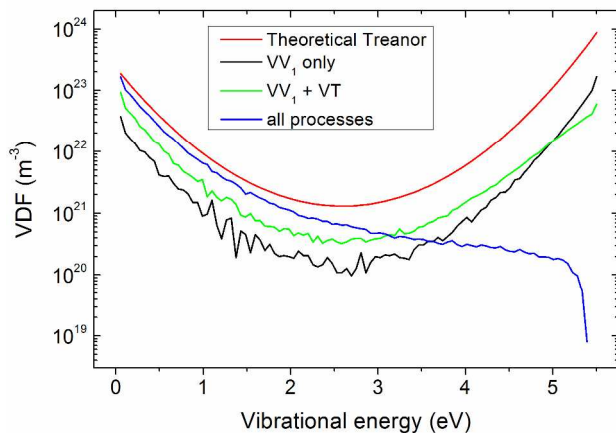


Figure 5. Vibrational distribution functions for $n_0 = 2.33 \times 10^{23} \text{ m}^{-3}$, $T_0 = 300 \text{ K}$ and $T_v = 0.25 \text{ eV}$, obtained for different choices of the boundary condition and processes. The theoretical Treanor distribution function (shifted upwards for better representation purposes) is also shown.

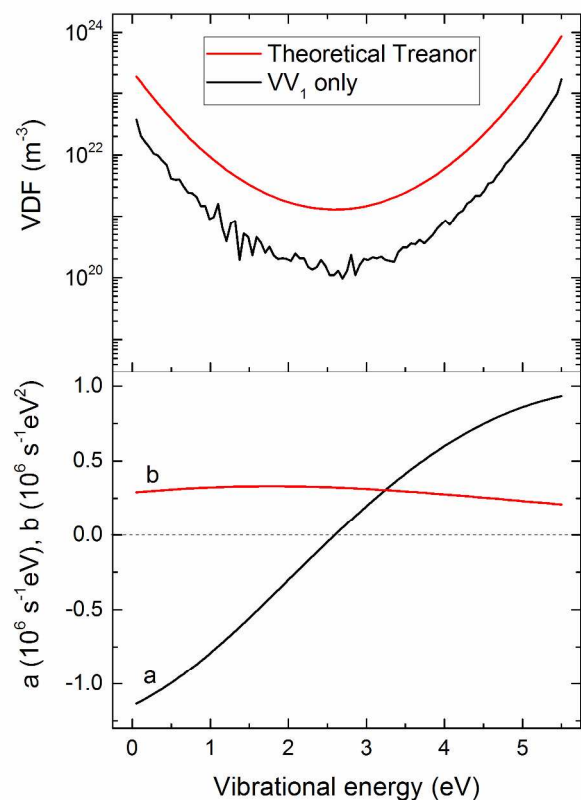


Figure 6. Vibrational distribution function with VV_1 processes only, that reproduces the Treanor distribution for $T_v = 0.19$ eV and a $T_0 = 300$ K (see Figure 5) (top) and corresponding coefficients a and b (bottom). In the top panel, the theoretical Treanor distribution function (shifted upwards for better representation purposes) is also shown.

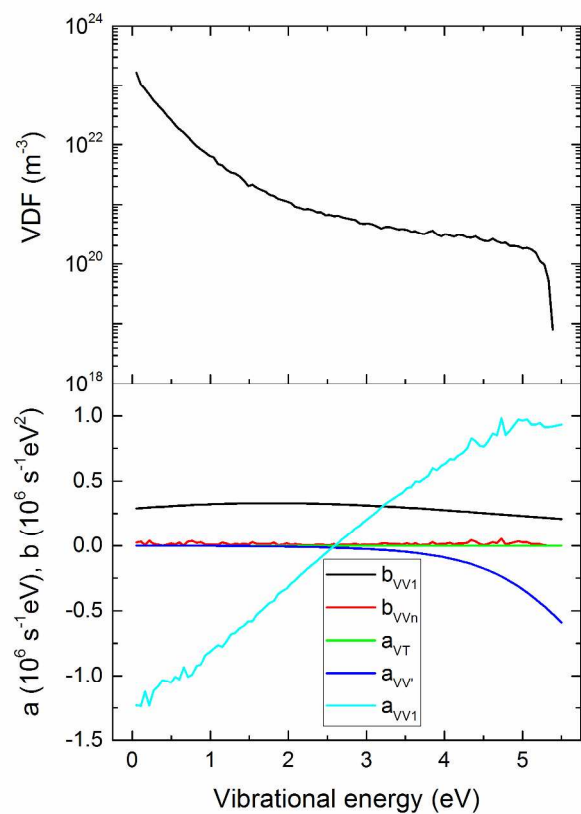


Figure 7. Vibrational distribution function with all the processes included ($T_v = 0.25$ eV and a $T_0 = 300$ K, see Figure 5) (top) and corresponding coefficients a and b (bottom).

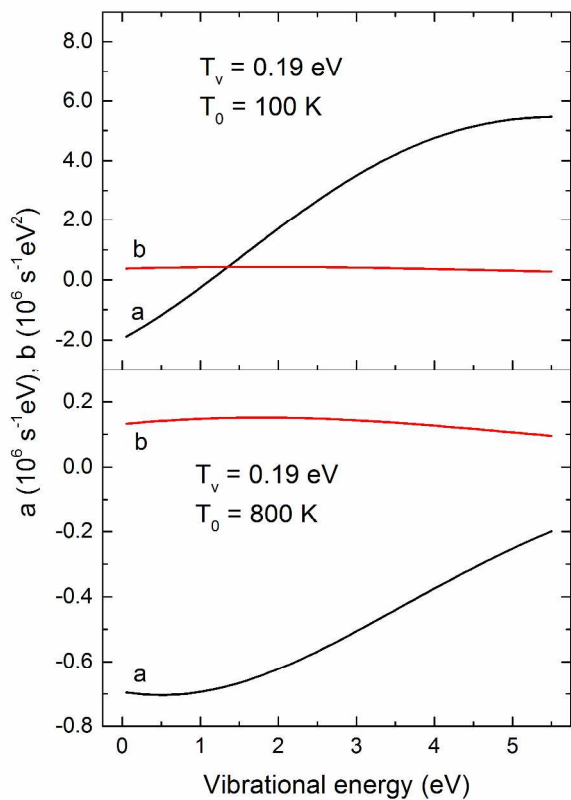


Figure 8. Coefficients a and b for the distribution with VV_1 processes only, for $T_v = 0.19$ eV and $T_0 = 100$ K (top) and 800 K (bottom).

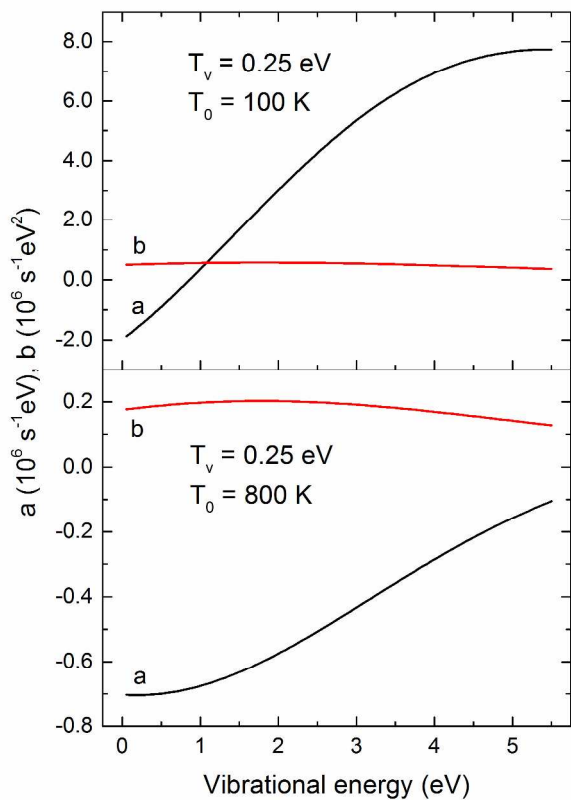
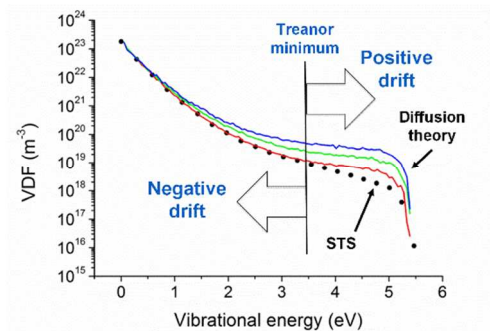
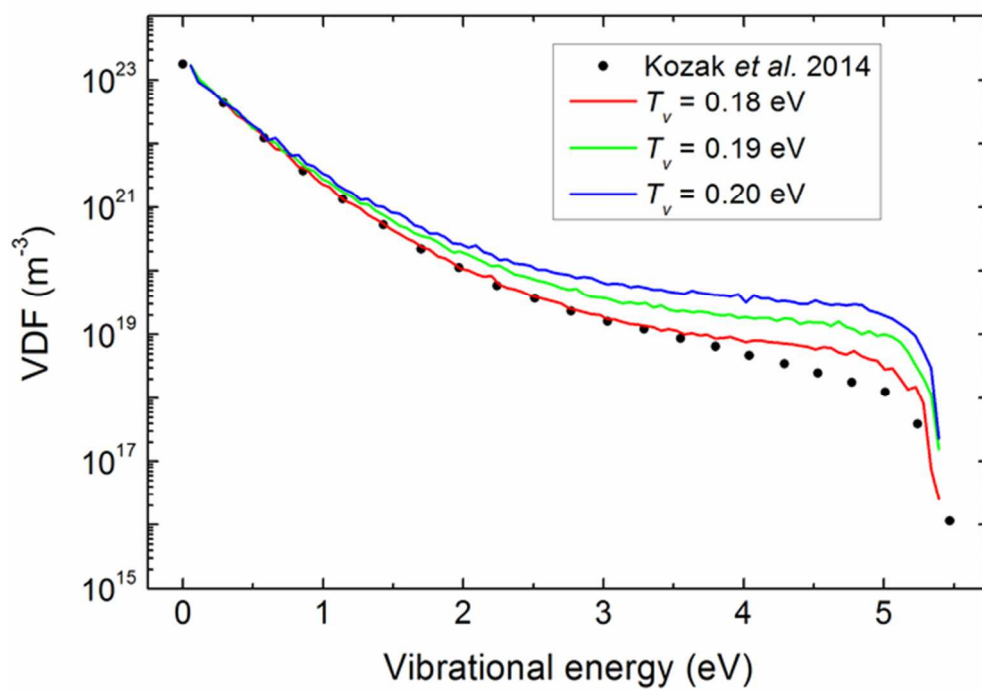


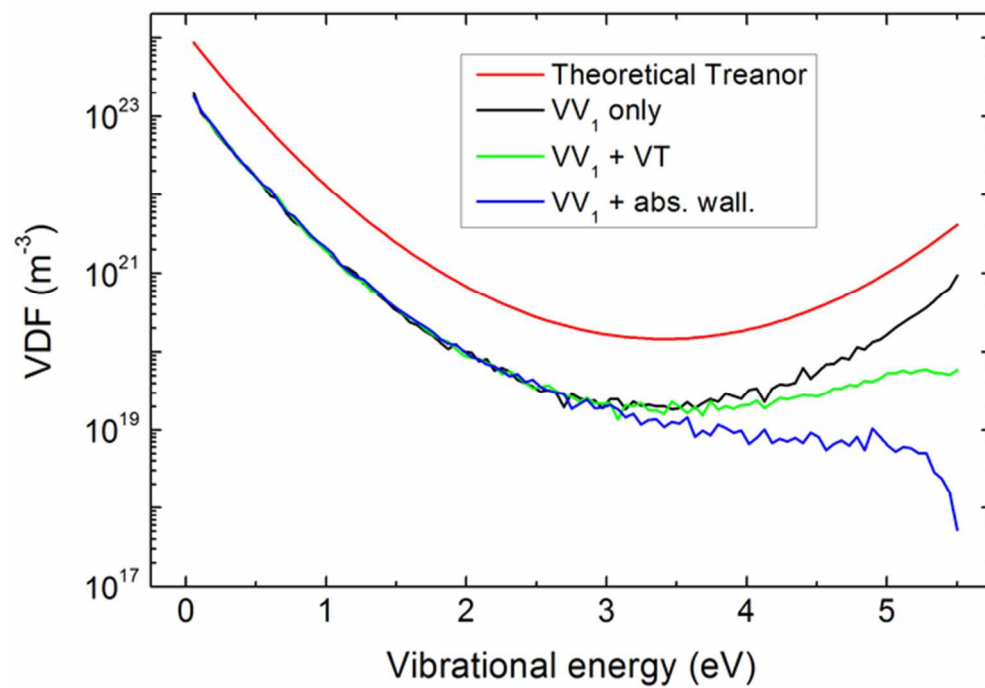
Figure 9. Coefficients a and b for the distribution with VV_1 processes only, for $T_v = 0.25$ eV and $T_0 = 100$ K (top) and 800 K (bottom).



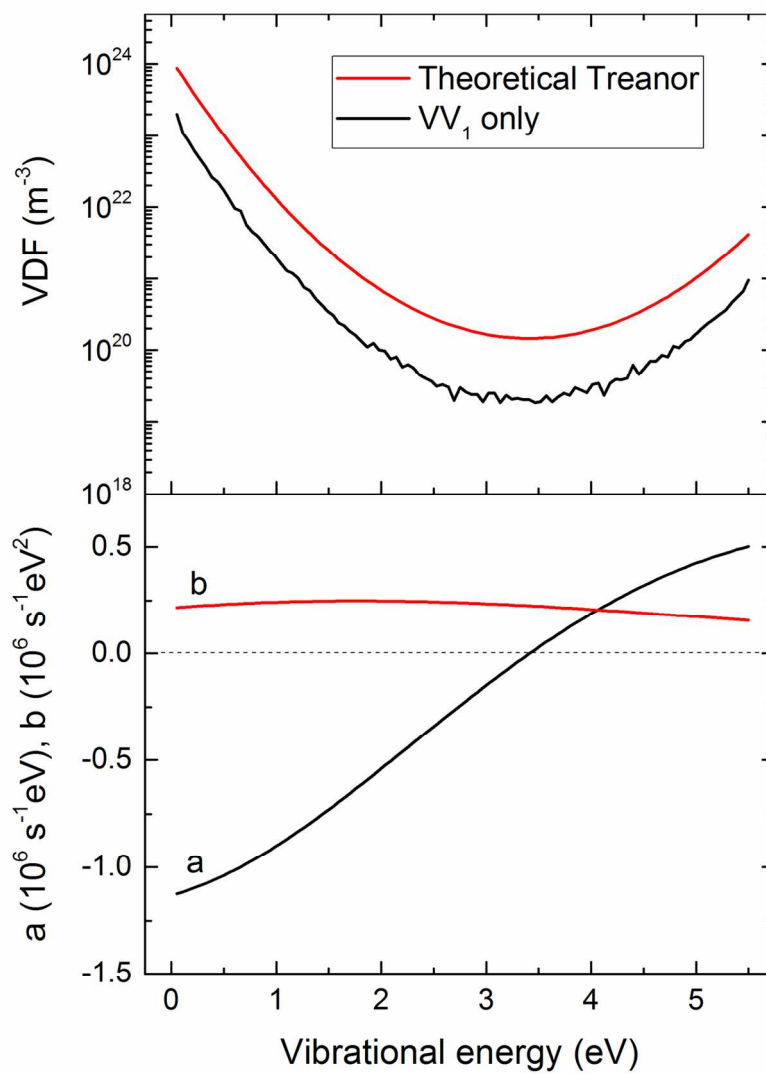
TOC Graphic



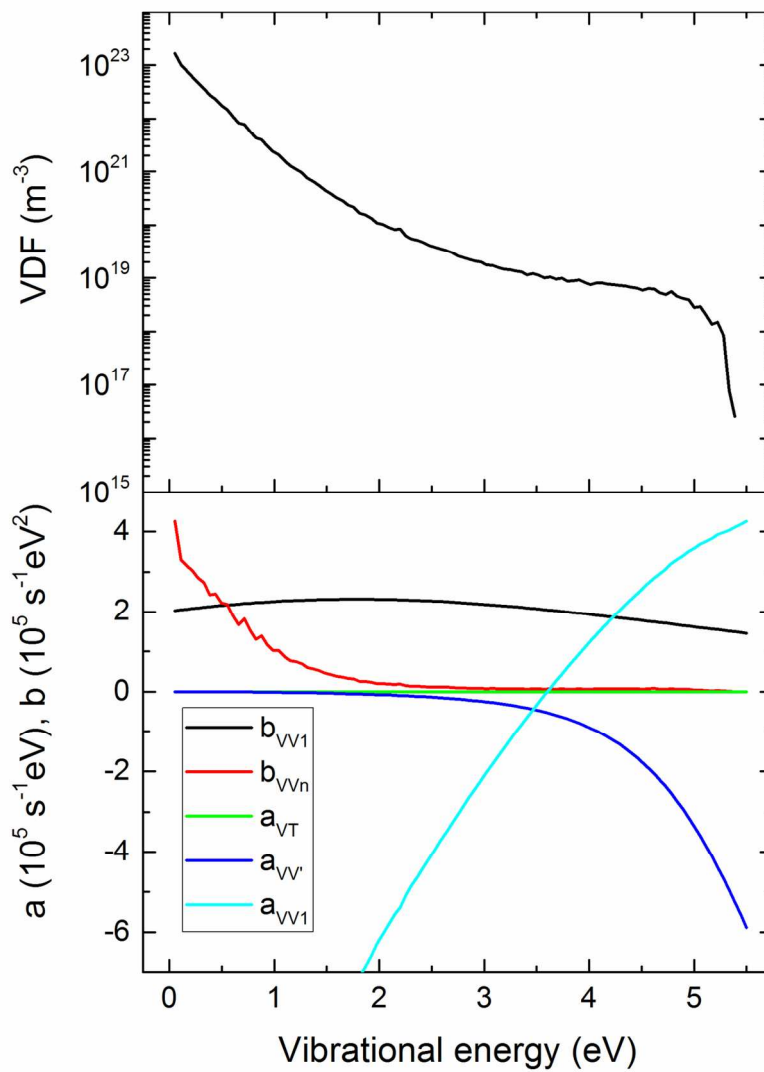
57x40mm (300 x 300 DPI)



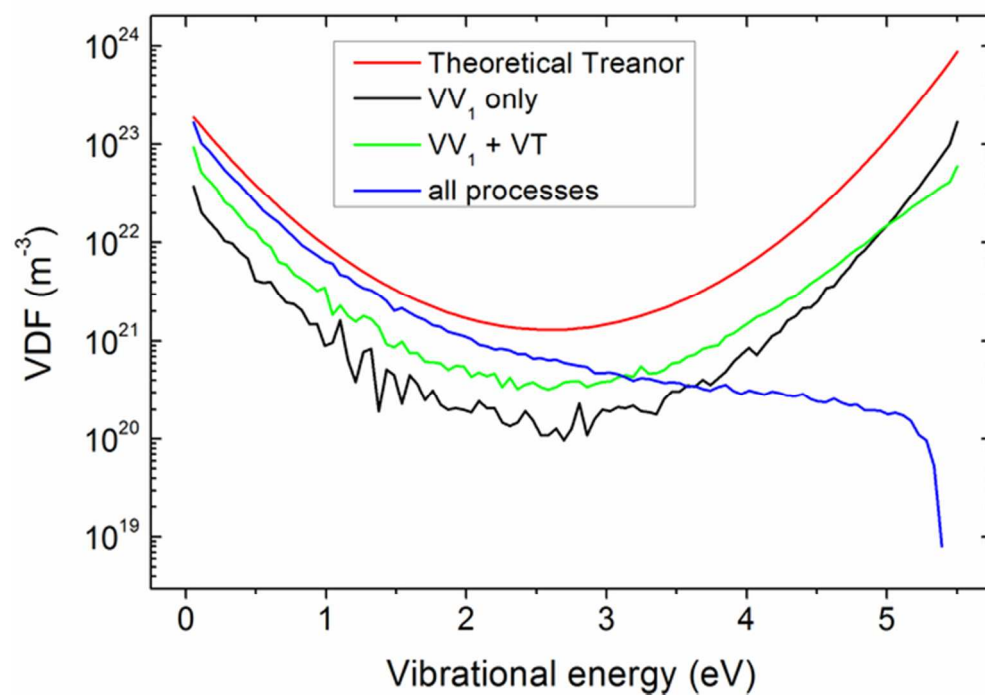
57x40mm (300 x 300 DPI)



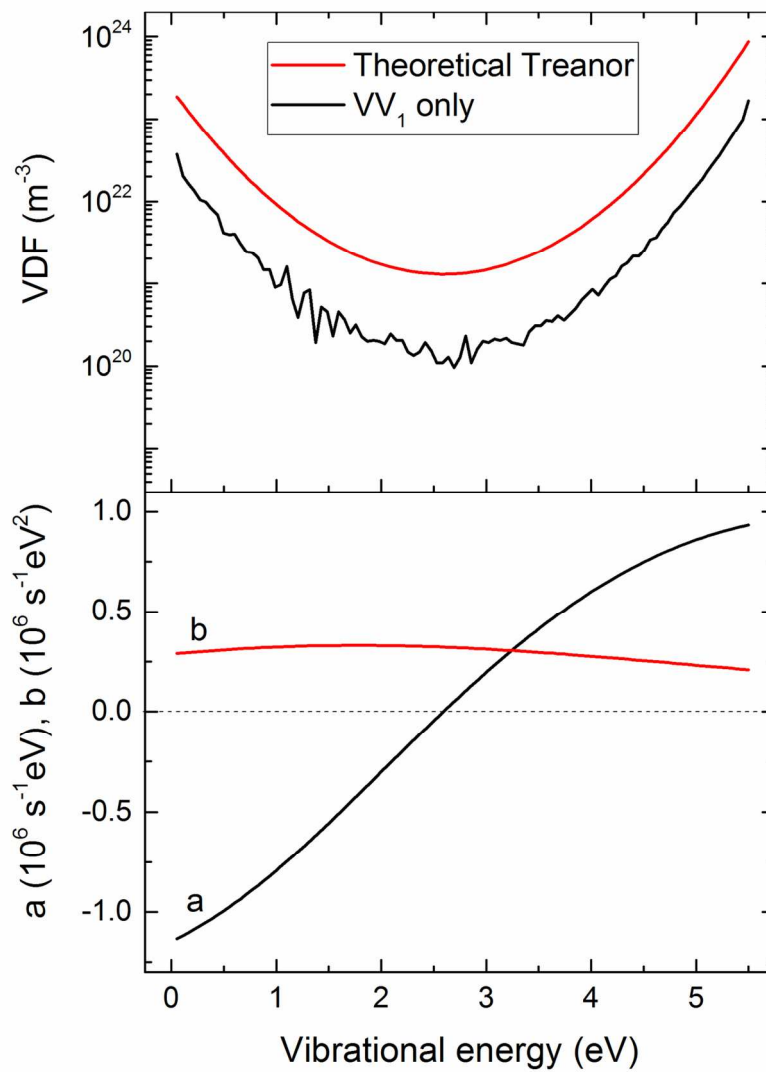
118x168mm (300 x 300 DPI)



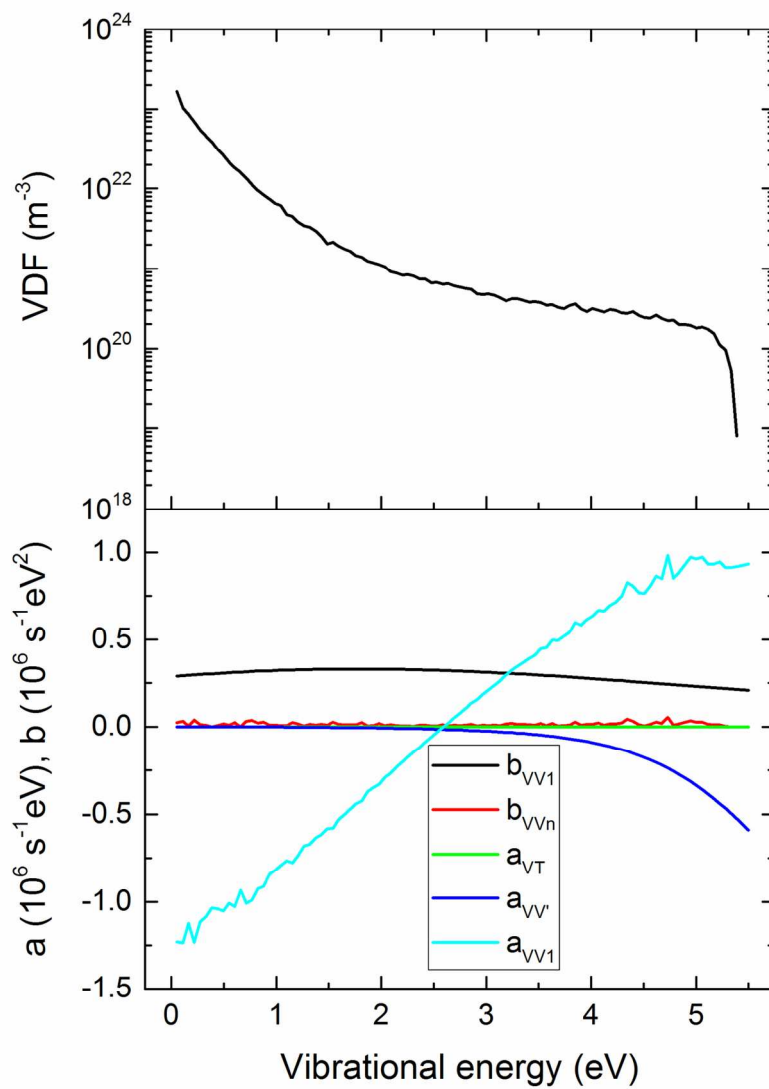
118x168mm (300 x 300 DPI)



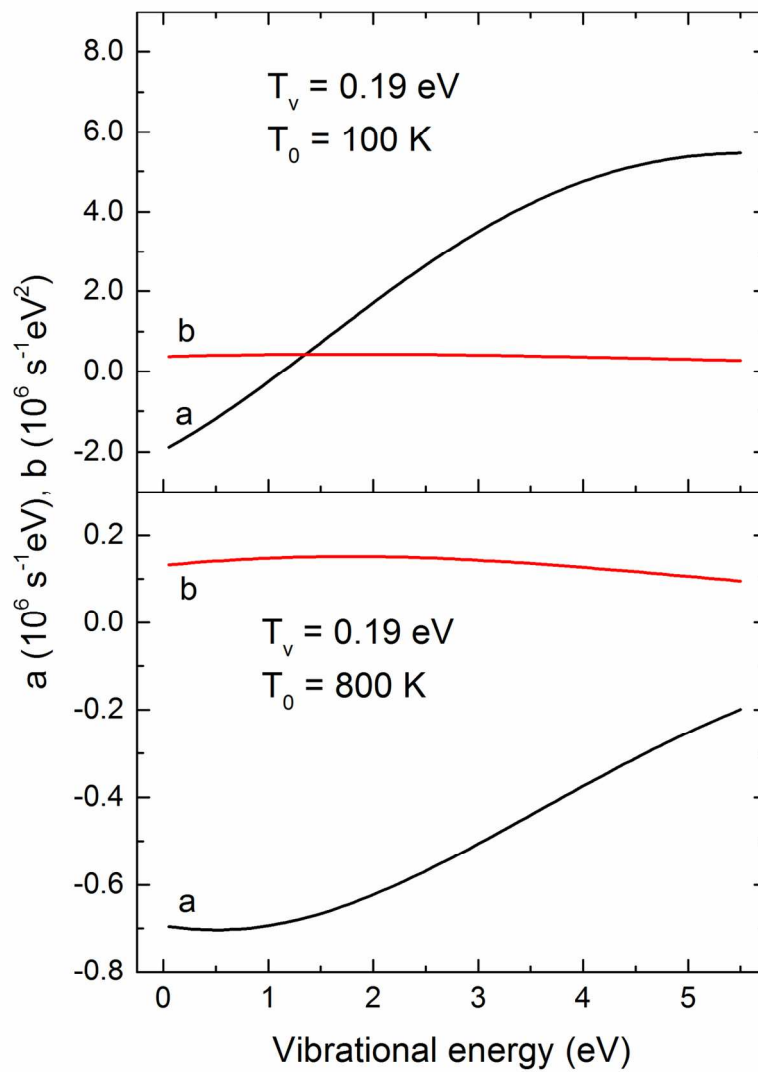
57x40mm (300 x 300 DPI)



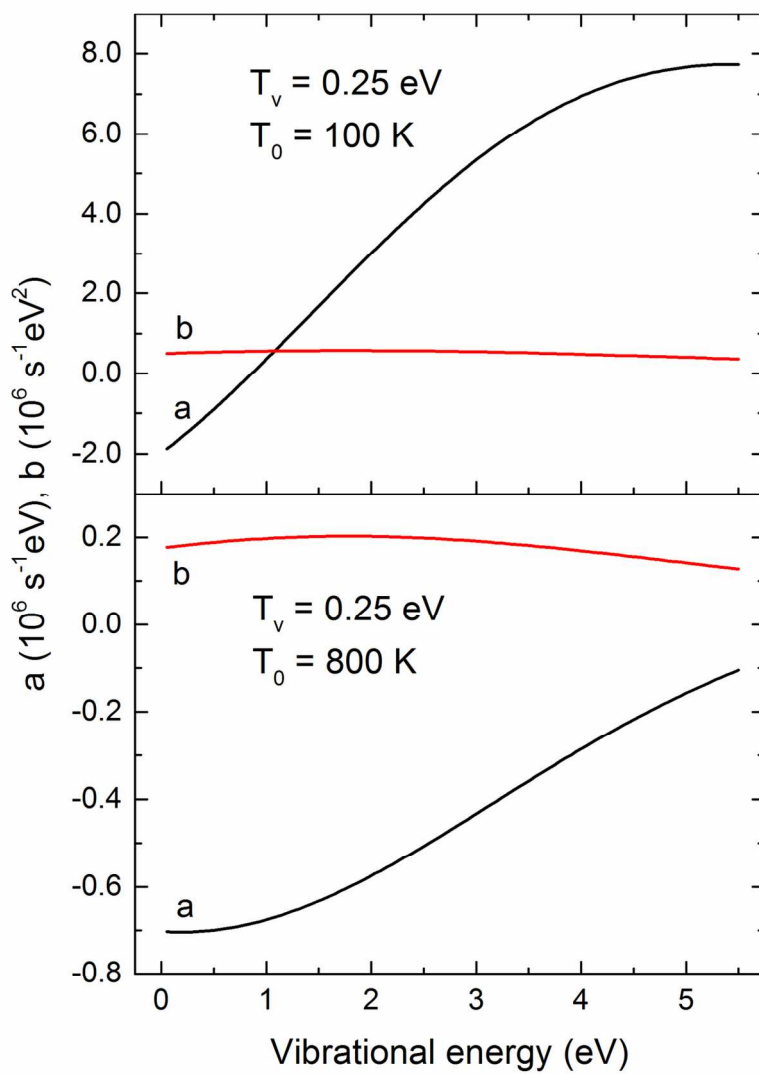
118x168mm (300 x 300 DPI)



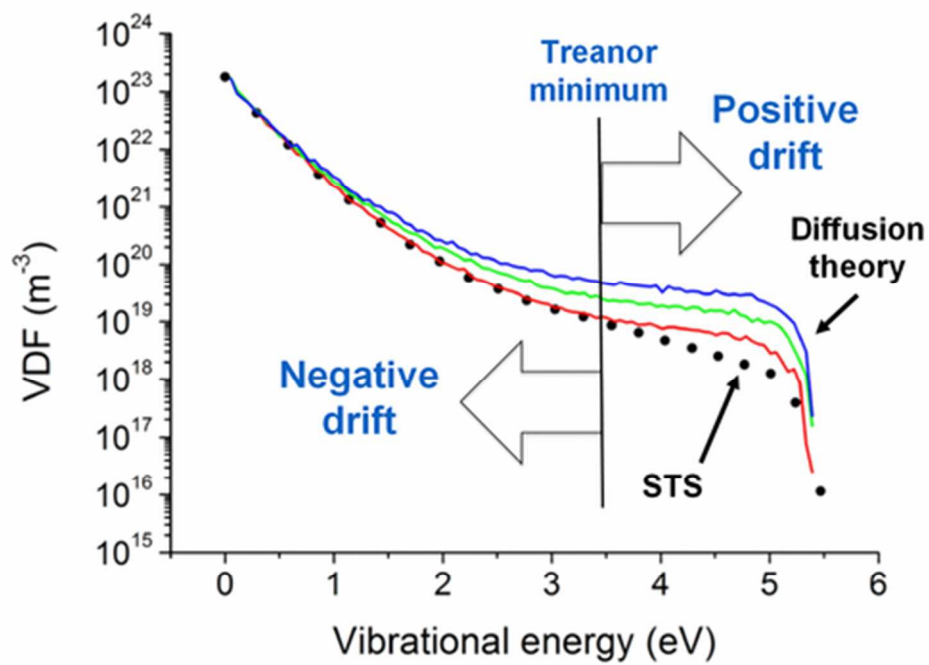
118x168mm (300 x 300 DPI)



118x168mm (300 x 300 DPI)



118x168mm (300 x 300 DPI)



44x30mm (300 x 300 DPI)